ILLINOIS INSTITUTE OF TECHNOLOGY

Planar laser-induced fluorescence imaging of fuel droplets exposed to asymmetric radiant heating

Illinois Institute of Technology
Mechanical, Materials and Aerospace Engineering Department
Advanced Thermal and Environmental Research Systems Laboratory

Kavin Ammigan

Fermilab Seminar
April 19th, 2012

research background

Fuel droplet vaporization

- Experimental/analytical work
- Radiative/convective heat transfer
- Mechanical design and solid modeling
- Laser based diagnostics
- Two-phase flow (liquid-gas)

Particle de-agglomeration (EPRI)

- Mercury emission reduction from coal power plants
- Experimental work
- Ultrasonic de-agglomeration
- Fluid shear nozzles
- Two-phase flow (solid-gas)

Summer Institute on Sustainability and Energy (UIC)

- Electrical smart grid
- Implementation of renewable energy
- Identification of social/economic barriers

Importance of droplet vaporization studies:

- critical parameter in designing combustion devices
- dictates residence time in combustion chamber
- determines when combustion takes place

where is asymmetric radiant heating common ?

- Conventional spray flames
- Counter-flow diffusion flames
- Spray periphery of conventional combustors
- Potential asymmetric heating from gases and soot in combustion chamber
- LIQUID-FUELED MICROCOMBUSTORS

microcombustors

- Uprising field in power generation
- Micro-electro mechanical systems (Power MEMS)
- Prototypes only tested with gaseous fuel

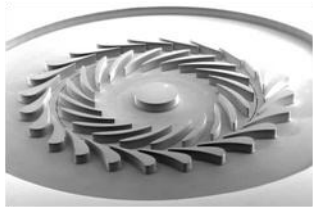

MIT 4mm diameter gas turbine (1997)

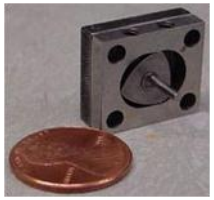

UC Berkeley mini rotary engine (1998)

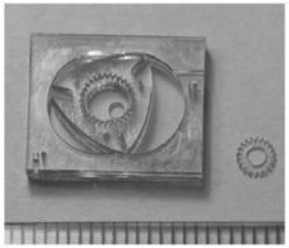

Uni. of Birmingham micro Wankel engine (2004)

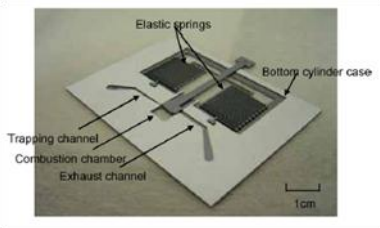

Ritsumeikan University MEMS ICE (2008)

High power density dependent on high mass flow rate of fuel: achievable with liquid fuels

microcombustors

- Uprising field in power generation
- Micro-electro mechanical systems (Power MEMS)
- Prototypes only tested with gaseous fuel

Device	**Power Density (MW/m^3)**
Micro Lithium Batteries	0.4
Micro Solar Cells	1
Micro Electric Motor	1.7
Micro Reactors (Si)	20
Large Scale Combustor	40
Micro Channel Reactors	150
Micro Magnetic Motors	200
Si Microcombustors	**2000**

High power density dependent on high mass flow rate of fuel: achievable with liquid fuels

Advantages of liquid fuel

- Higher power densities
- Smaller storage volumes (liquid-to-vapor density ratios of 500-700)
- Longer refueling intervals

Development challenges

- Liquid fuel delivery
- Need for rapid fuel vaporization and mixing
- Increased property gradients

1. Strong velocity gradient
2. Asymmetric heat fluxes
3. <u>Asymmetric thermal radiant heating</u>

thermal radiation consideration

- Microcombustor fabrication: silicon and silicon compounds
  - High emissivity: silicon compounds **(0.84-0.87)** conventional iron alloy combustors **(0.14-0.30)**
- High surface area-to-volume ratio
  - High heat loss rates

→ 2 orders of magnitude larger than conventional combustors (Spadaccini, 2007)

- Insulation required for microcombustor walls
  - Increase in wall temperature

High emissivity + High wall temperatures = Asymmetric radiant heating

objectives of study

- **Experimental investigation**
  - PLIF imaging of monodisperse stream of droplets irradiated by infrared panel
- **Thermal radiation absorption model**
  - Geometrical optics model with complex refractive index spectra of liquid components

experimental method

Planar Laser-Induced Fluorescence

- Laser beam converted into a sheet and illuminates flow of interest
- Tracer species excited by laser
- Resulting fluorescence signals captured on camera

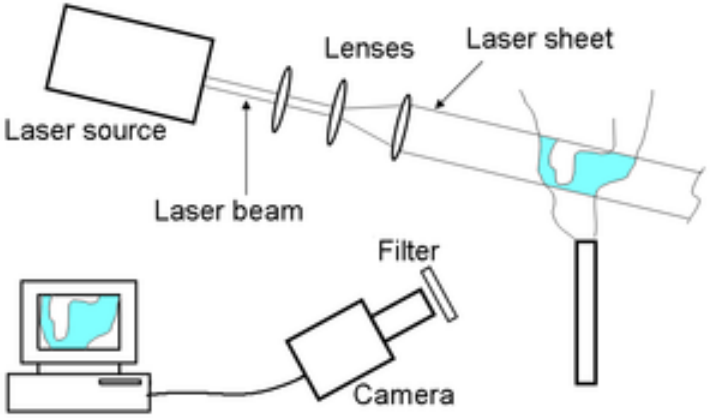

tracer: acetone

- Absorption spectrum: 225 nm to 320 nm
- Fluorescence emission: 350 nm to 550 nm
- Fluorescence lifetime: 4 ns
- Chemically stable up to 1000 K
- High vapor pressure at room temperature (easy seeding)
- High fluorescence signals

PLIF diagnostic components

- Laser system: Nd:YAG at 266 nm
- EMCCD camera (Electron Multiplying Charged Couple Device)
- UV camera lens and filters (for $350 < \lambda < 550$ nm transmission)
- UV grade optical lenses
  - Plano-concave (f = -19 mm)
  - Symmetric convex lens (f = 120 mm)

acetone PLIF calibration

$$S_f \propto \frac{\chi_{acetone} P \lambda}{T}$$

S_f	Fluorescence signal
λ	Excitation wavelength
$X_{acetone}$	Acetone mole fraction
P	Pressure
T	Temperature

Fluorescence signal S_f :

1. proportional to acetone mole fraction (P, T and λ constant)
2. inversely proportional to temperature (P, λ and $X_{acetone}$)
3. proportional to pressure (T, λ and $X_{acetone}$)

acetone PLIF calibration

$$S_f \propto \frac{\chi_{acetone} P \lambda}{T}$$

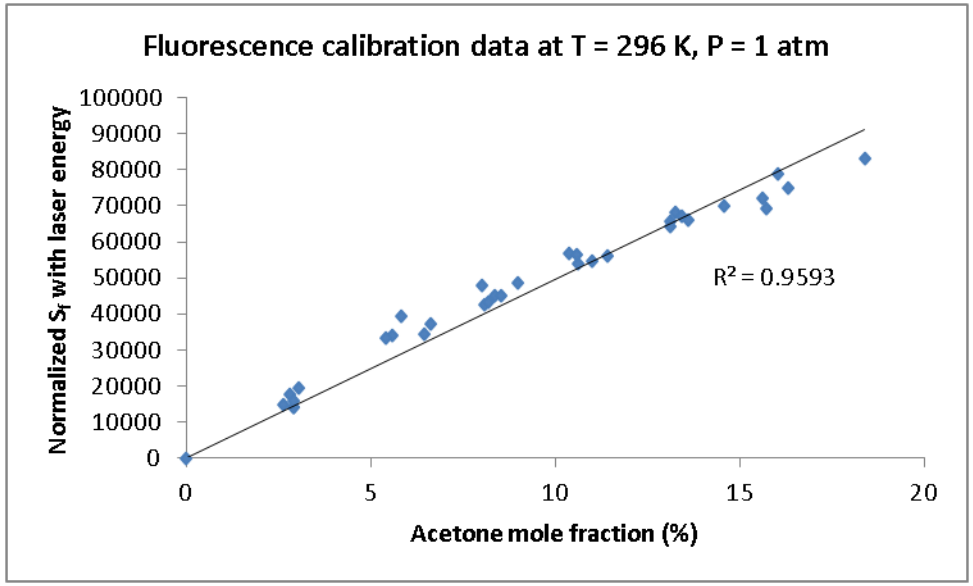

(Ammigan, 2007)

Temperature dependence data (Thurber, 1999)

λ = 266 nm	
T(K)	**S^*_f**
296	1.000
329	0.880
374	0.770
424	0.660
483	0.552

S^*_f Measured relative fluorescence per unit acetone mole fraction

asymmetric radiant heating set-up

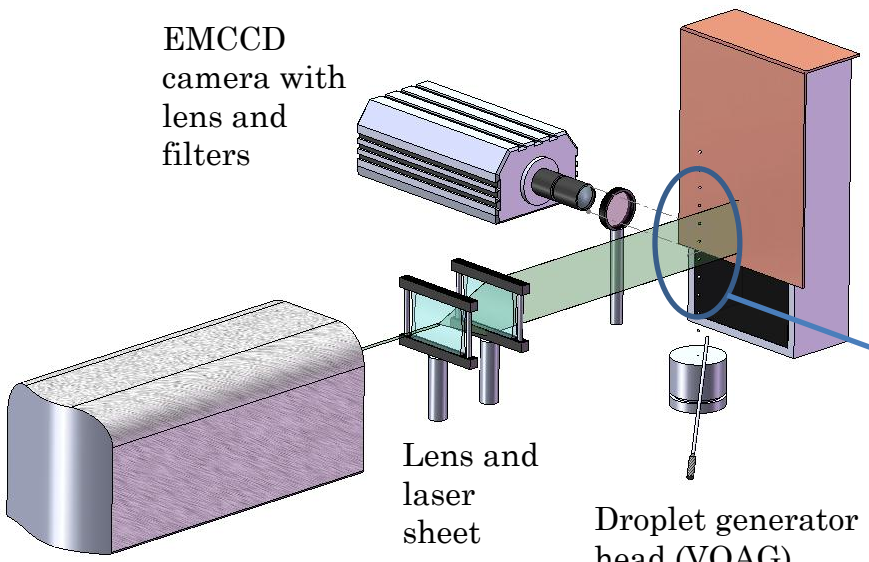

Contour plot of acetone mole fraction around a droplet

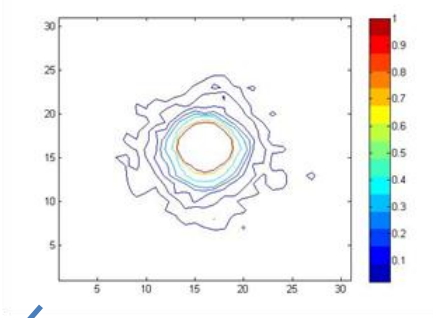

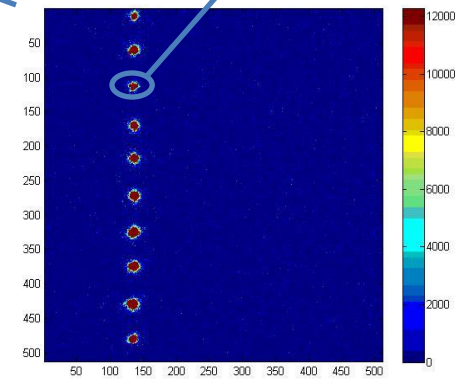

Raw fluorescence image of droplet stream at 296 K

experimental conditions

- Pure and bi-component (1:1 volume ratio) droplets
  - Alkanes: **octane** and **hexane**
  - Alcohols: **ethanol** and **2-propanol**

Properties	Acetone	Hexane	Octane	Ethanol	2-propanol
Boiling point (K)	330	342	399	351	355
Latent heat (kJ/mol)	30.1	30.7	34.6	38.97	43.9
Specific heat (kJ/kg.K)	2.15	2.26	2.15	2.46	2.56
Density (kg/m^3)	790	655	703	789	785
Molecular weight (kg/kmol)	58.08	84.16	114.23	46.07	60.1

experimental conditions

- Pure and bi-component (1:1 volume ratio) droplets
  - Alkanes: **octane** and **hexane**
  - Alcohols: **ethanol** and **2-propanol**

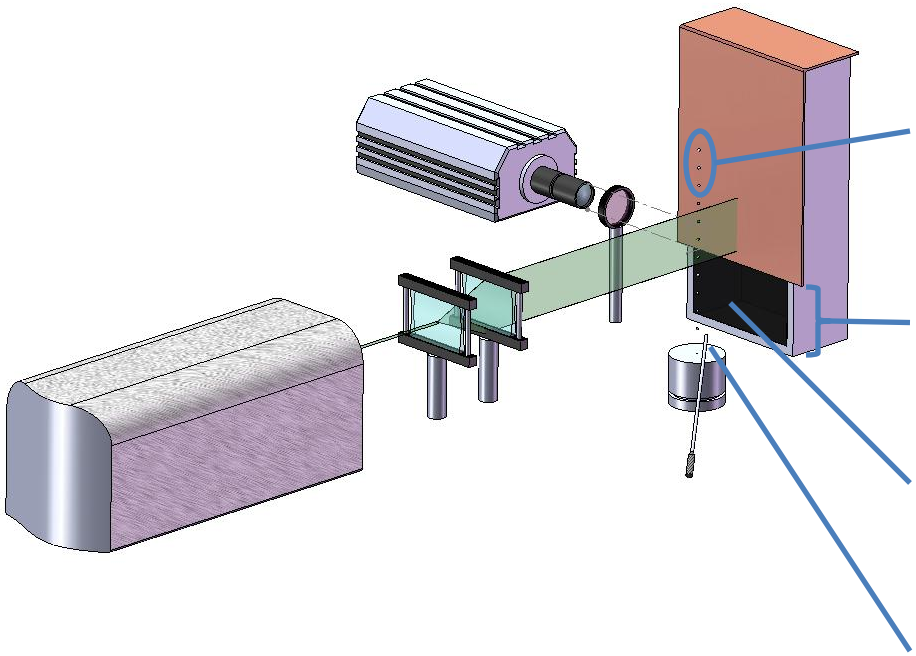

- Droplet diameters: 145, 158, 193, 235 μm
- Exposure length of 5.5 cm
- Panel heater surface temperatures: 455 K (2400 W/m^2) and 475 K (2900 W/m^2)
- Droplet stream axis temperatures: 322 K and 333 K
- Ambient pressure: 1 atm

experimental results

contour plots

*Acetone/**Hexane** bi-component droplets, D = 145 μm*

No radiant heating | 455 K | 475 K

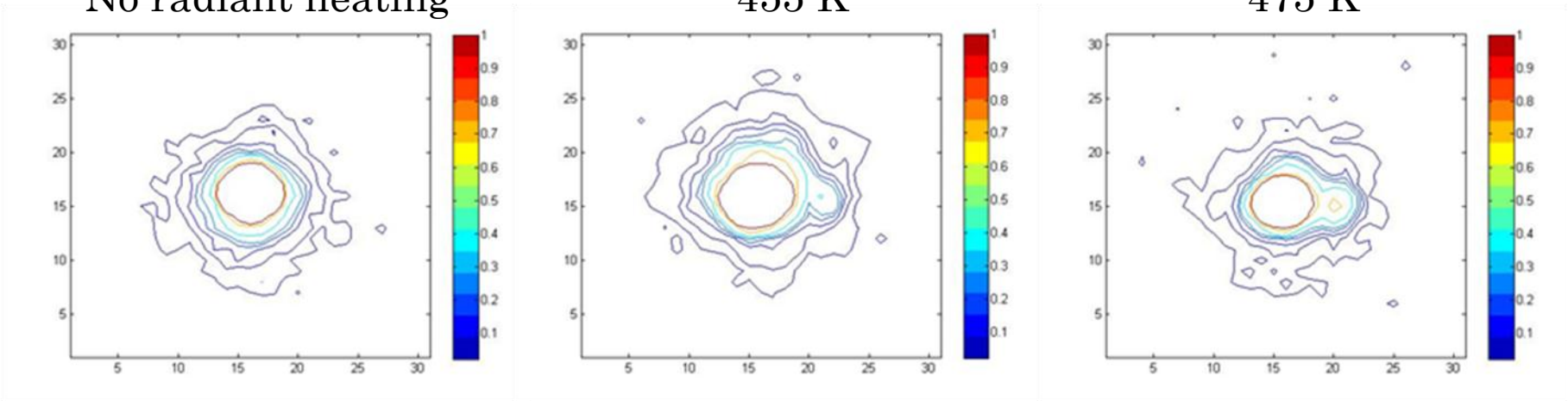

- Laser sheet propagating from left to right
- Right side of droplet irradiated by IR panel heater
- Colorbar represents acetone mole fraction, X
- Pixel values on x and y axes (1 pixel = 17.5 μm)
- Highly localized surface vaporization induces asymmetric Stefan flow

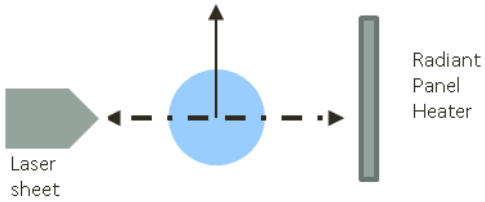

radial vapor distribution

*Acetone/**Alkanes** bi-component droplets, D = 193 μm*

No radiant heating

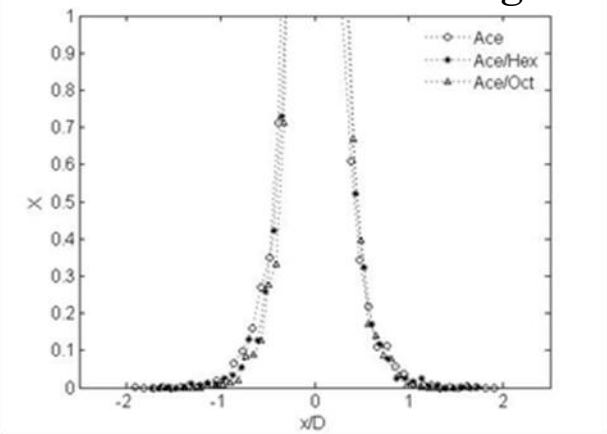

455 K

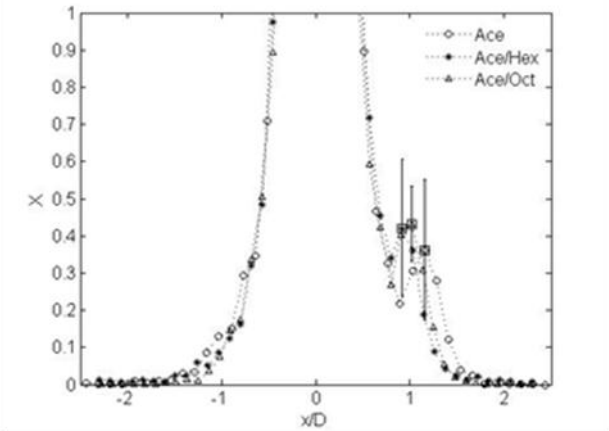

475 K

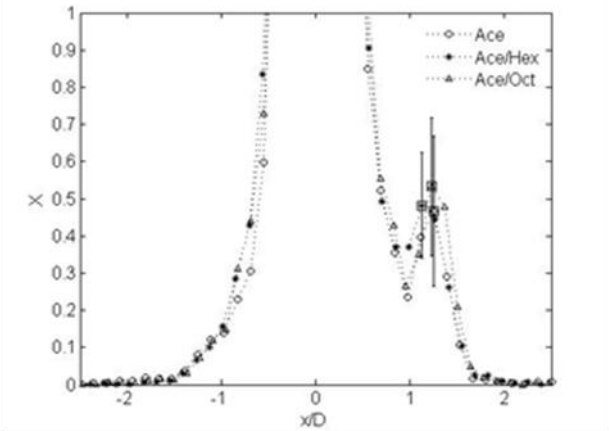

- Acetone mole fraction (X) against normalized radial distance (x/D)
- Each graph is an average of 10 droplets
- Error bars: ± 1 standard deviation

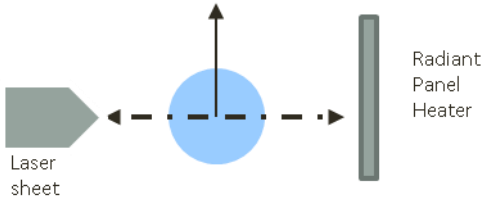

data interpretation

droplet convective model

- Droplets are exposed to both convective and radiant heating
- Convective effects analyzed using a droplet vaporization model (Miller, 1998; Varanasi, 2004)
    - Simulates droplets in an isothermal air flow (axisymmetric)
    - Droplet stream axis temperature of 322 K and 333 K
- Input data into model:
    - Droplet composition and volume fraction
    - Droplet initial temperature (296 K)
    - Ambient air temperature (droplet stream axis temperature)
    - Droplet diameter
    - Reynolds number (based on exit velocity from VOAG)

Pure and bi-component 193 μm droplets at droplet stream axis temperature of 333 K

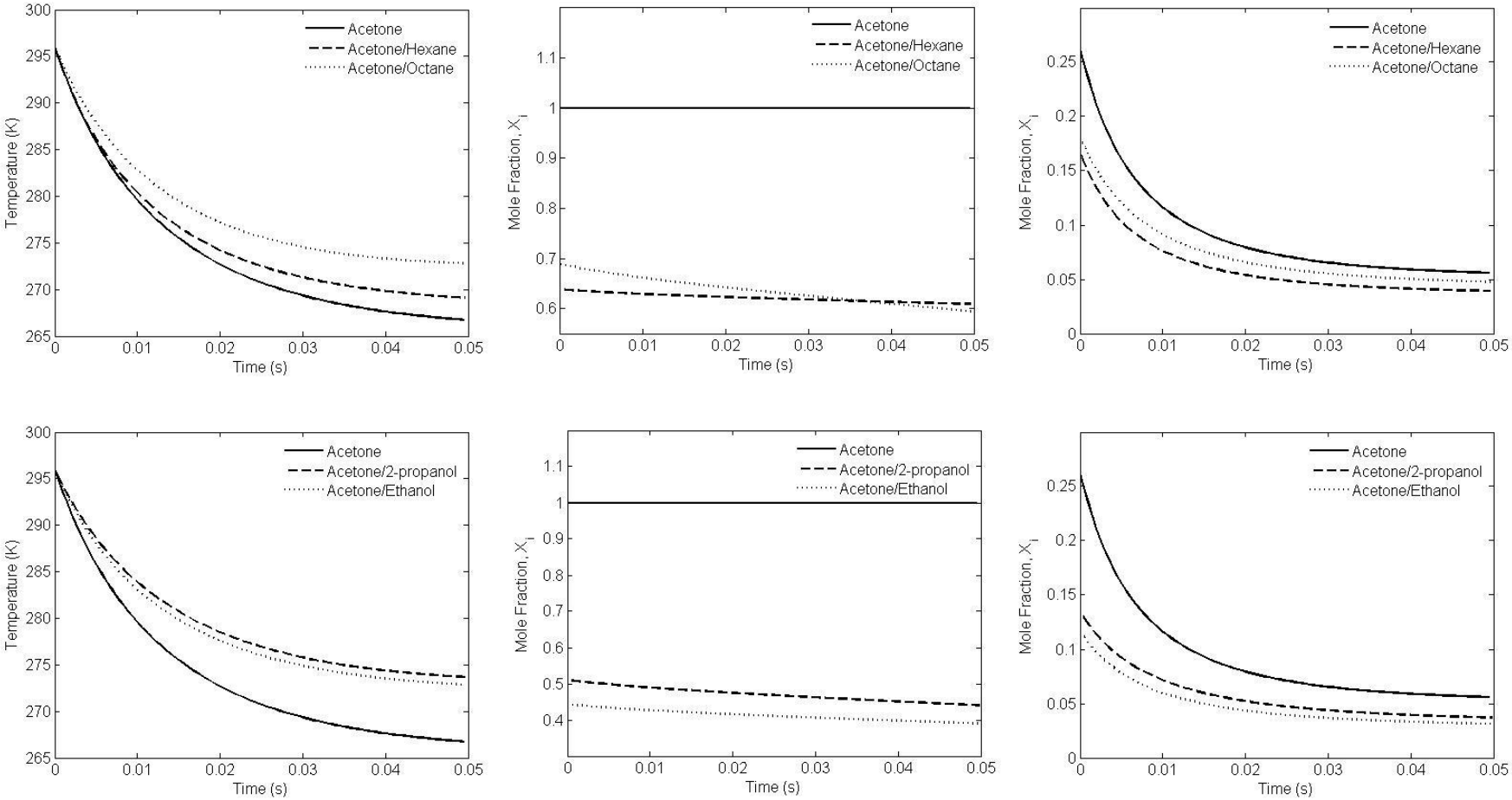

Average droplet temperature

Acetone mole fraction in bulk liquid droplet

Acetone vapor mole fraction at droplet surface

droplet radiation absorptivity – geometrical optics model

- *Absorptivity*: fraction of incident thermal radiation absorbed by droplets

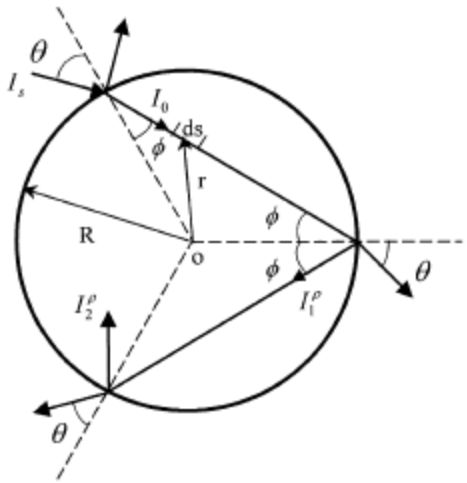

Physical geometry of the system and ray tracing (Viskanta, 2005; Liu, 2002)

- Transmission and reflection at gas-liquid interface
- Internal reflections within droplet
- Input data: **complex refractive index spectrum of each component**

$$\tilde{n_\lambda} = n_\lambda + ik_\lambda$$

- Wavelength range: 2.5 μm < λ < 15 μm
- Spectrum obtained from Dr. Keefe (Cape Breton University) and Dr. Bertie (University of Alberta)

complex refractive index spectra

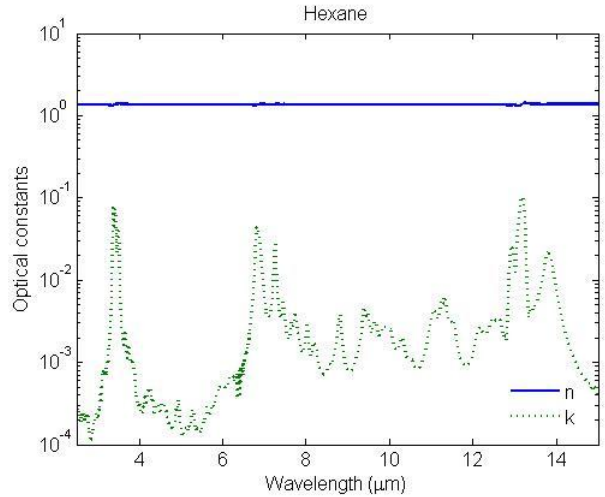

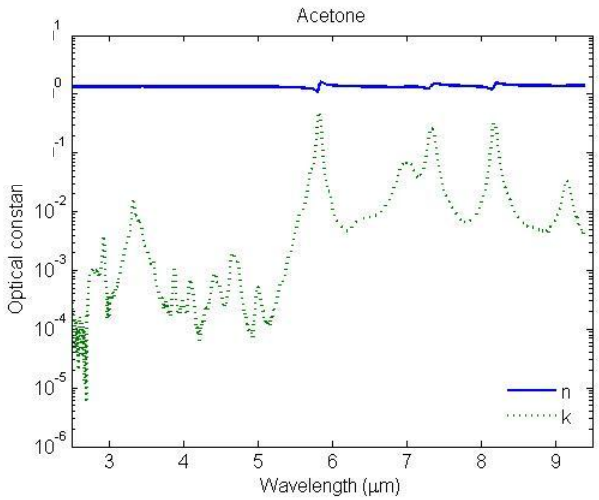

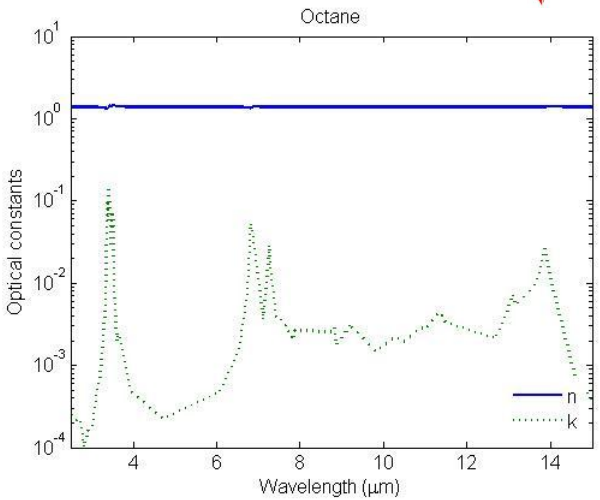

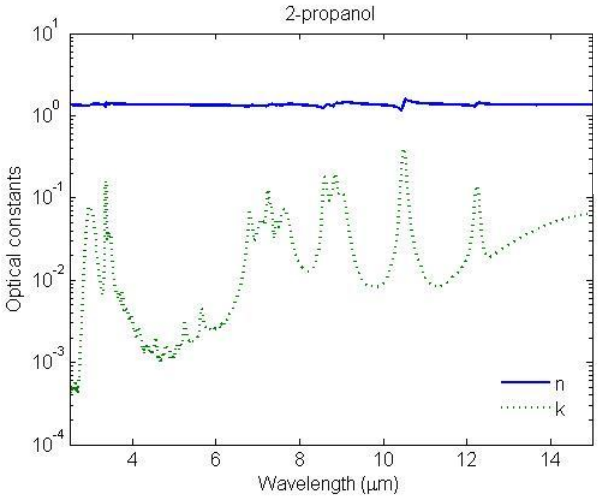

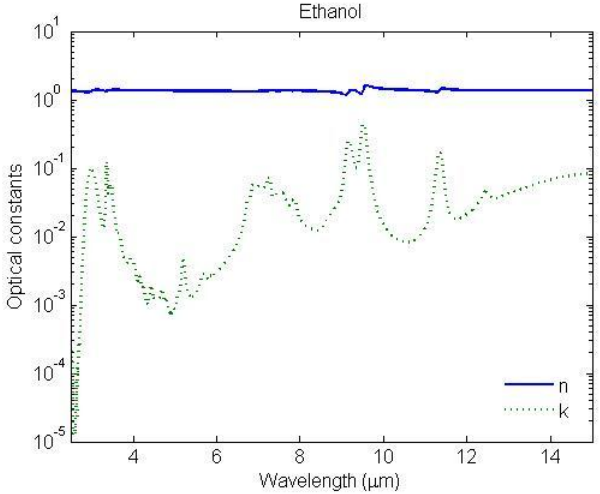

Bertie (2009), Keefe (2005, 2009)

Total spectral absorptivity

$$\alpha_\lambda = \int_0^{\pi/2} \frac{[1-\rho_\perp(\theta)][1-exp(-4xk_\lambda \cos\phi)]}{1-\rho_\perp(\theta)exp(-4xk_\lambda \cos\phi)} + \frac{[1-\rho_\parallel(\theta)][1-exp(-4xk_\lambda \cos\phi)]}{1-\rho_\parallel(\theta)exp(-4xk_\lambda \cos\phi)} \sin\theta\cos\theta d\theta$$

Spectral blackbody emissive power of radiant panel heater

$$E_{\lambda,b}(\lambda,T) = \frac{C_1}{\lambda^5[exp(C_2/\lambda T)-1]}$$

Total absorptivity

$$\alpha = \frac{\int_{\lambda_1}^{\lambda_2} \alpha_\lambda(\lambda)\cdot E_{\lambda,b}(\lambda,T)\cdot d\lambda}{\int_{\lambda_1}^{\lambda_2} E_{\lambda,b}(\lambda,T)\cdot d\lambda}$$

Total absorptivity dependent on : panel temperature, droplet diameter and liquid composition

absorptivity values

T (K)	Acetone		Hexane		Octane		2-propanol		Ethanol	
	455	475	455	475	455	475	455	475	455	475
D (μm):										
145	0.578	0.573	0.294	0.291	0.323	0.321	0.750	0.741	0.766	0.757
158	0.596	0.591	*	*	*	*	0.764	0.755	0.782	0.773
193	0.637	0.631	0.348	0.344	0.383	0.380	0.792	0.785	0.804	0.796
235	0.676	0.669	0.387	0.383	0.426	0.423	0.820	0.814	0.826	0.819

- Absorptivity of bi-component mixtures varies non-linearly with composition (Chapados and Max, 2007)

Droplet diameter increases → α increases
Radiant panel temperature increases → α decreases

peak acetone mole fraction and integrated area

- Average integrated areas under the peak
- Average values of the peak acetone mole fraction
- Measured bi-component areas and peak mole fraction scaled by initial mass of acetone evaporated

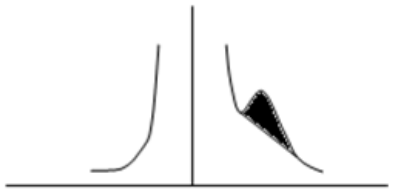

193 μm and 235 μm droplets irradiated at 475 K

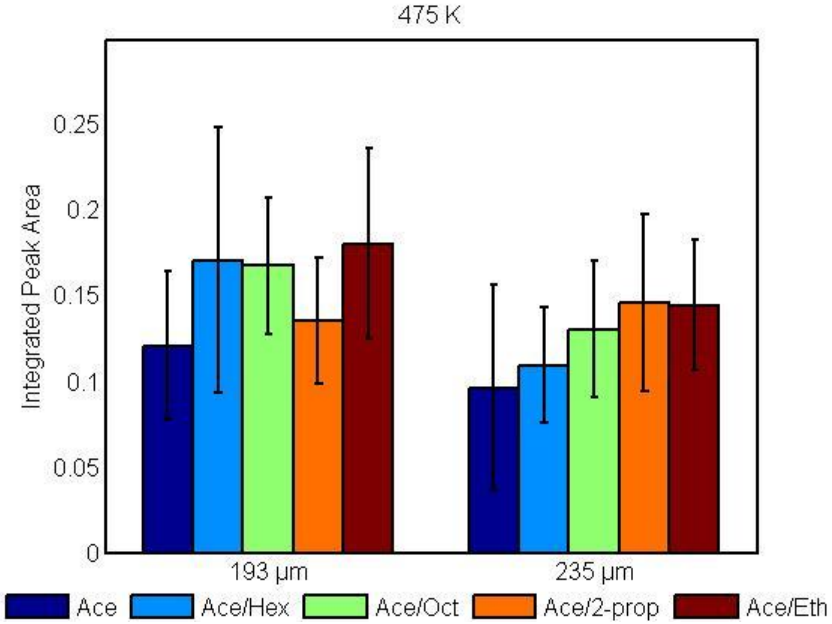

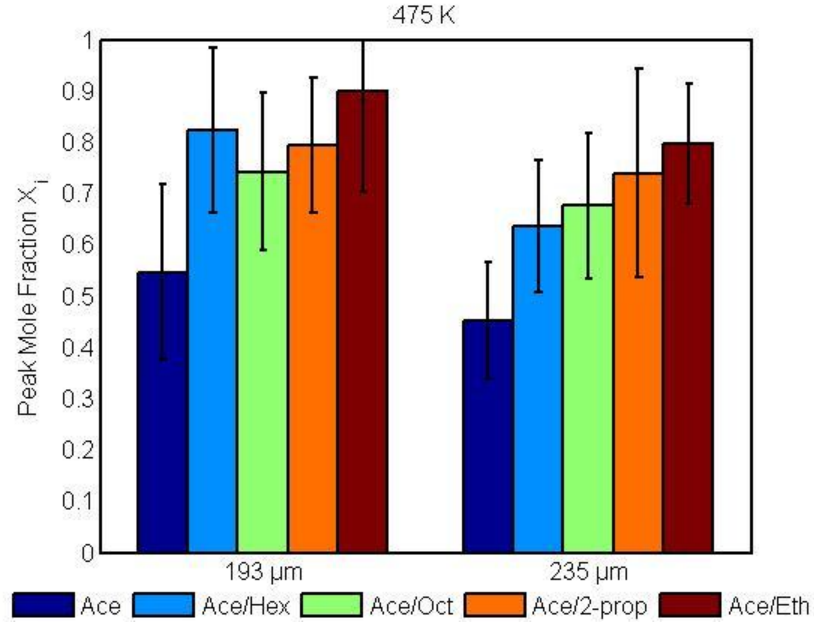

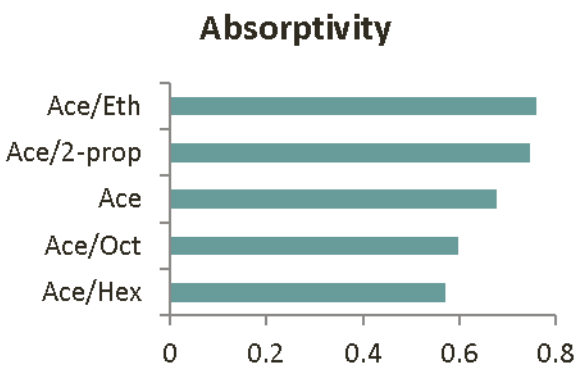

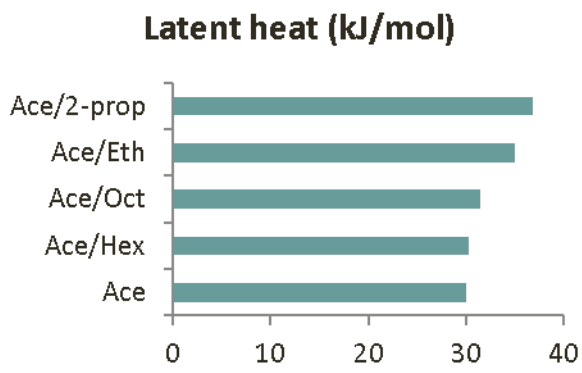

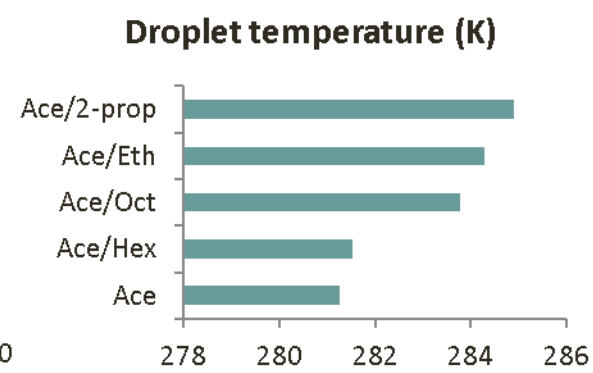

effects of D & T on total absorptivity

- Geometrical optics model

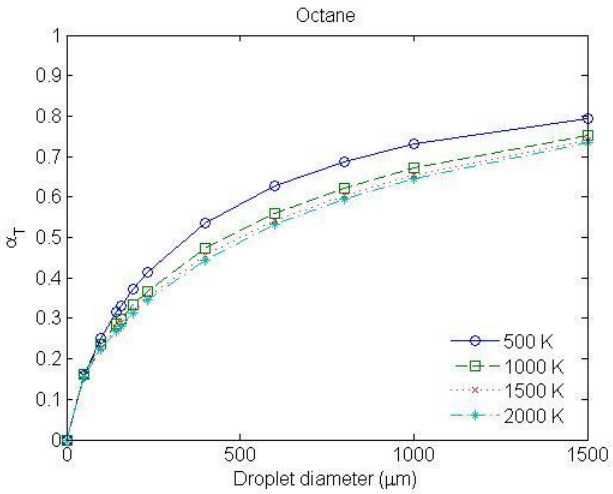

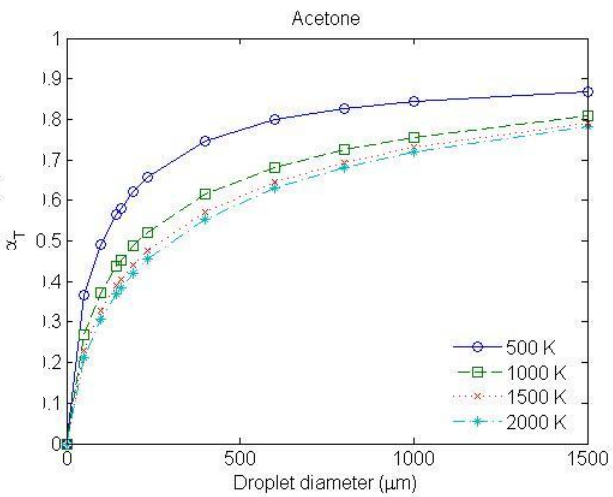

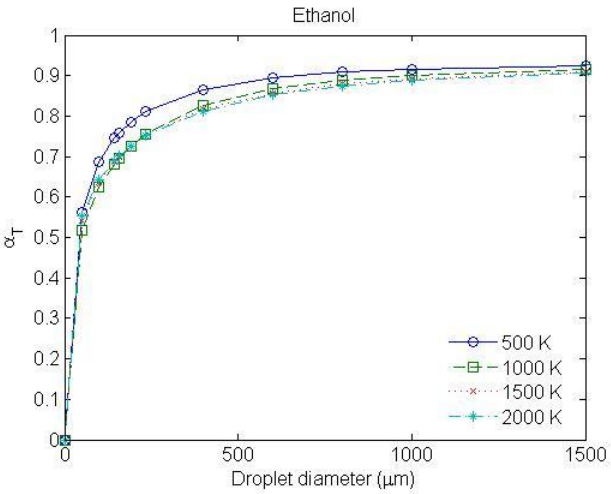

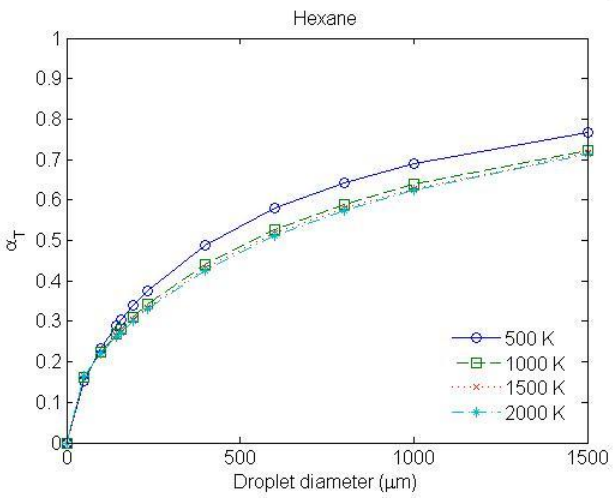

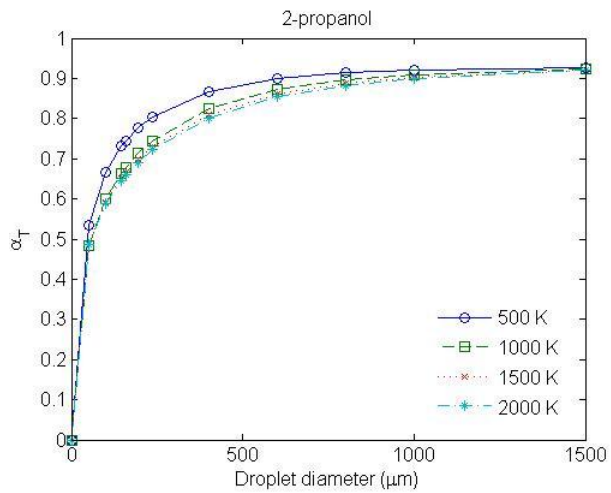

Typical operating conditions of combustion devices

Device	Diameter range (μm)	Wall temperature (K)
Gas turbine	10 – 400	500 – 1000
Typical ICE	20 – 200	450 – 500
Micro gas turbine	20 - 100	600 – 750
Microcombustor	1 - 100	600 - 750

- Diameter range of 1 – 400 μm
  - 800 % increase in alcohol absorptivity
  - 600 % increase in acetone absorptivity
  - 500 % increase in alkane absorptivity
- Temperature change of 500 K
  - Less than 10 % change in absorptivity
- Absorptivity highly sensitive to diameter change

internal distribution of radiation absorption

Spectral radiation absorption (W/µm)

$$Q(y) = 4\pi^2 R^2 I_s \int_0^{\theta_{end}} \{exp[-2xk_\lambda(\cos\phi - \sqrt{y^2 - \sin^2\phi})] - exp[-2xk_\lambda(\cos\phi + \sqrt{y^2 - \sin^2\phi})]\} \cdot \sin\theta\cos\theta \times \left\{ \frac{[1-\rho_\perp(\theta)]}{[1-\rho_\perp(\theta)exp(-4xk_\lambda\cos\phi)]} + \frac{[1-\rho_\parallel(\theta)]}{[1-\rho_\parallel(\theta)exp(-4xk_\lambda\cos\phi)]} \right\} d\theta$$

Local volumetric **spectral** radiation absorption

$$q_V(y) = \frac{dQ(y)}{4\pi r^2 dr}$$

Total local volumetric radiation absorption

$$q_V^T(y) = \int_{\lambda_1}^{\lambda_2} q_V(y) d\lambda$$

Average volumetric **spectral** radiation absorption

$$q_V^{av} = \frac{4\pi^2 R^2 I_s \alpha_\lambda}{4/3\pi R^3}$$

Total average volumetric radiation absorption

$$q_V^{av,T} = \int_{\lambda_1}^{\lambda_2} q_V^{av} d\lambda$$

Local dimensionless volumetric **spectral** radiation absorption

$$\beta(y) = \frac{q_V(y)}{q_V^{av}}$$

Total local dimensionless volumetric radiation absorption

$$\beta^T(y) = \frac{q_V^T(y)}{q_V^{av,T}}$$

effects of D & T on $\beta^T(y)$

$\beta^T(y)$ – Total local dimensionless volumetric radiation absorption

acetone

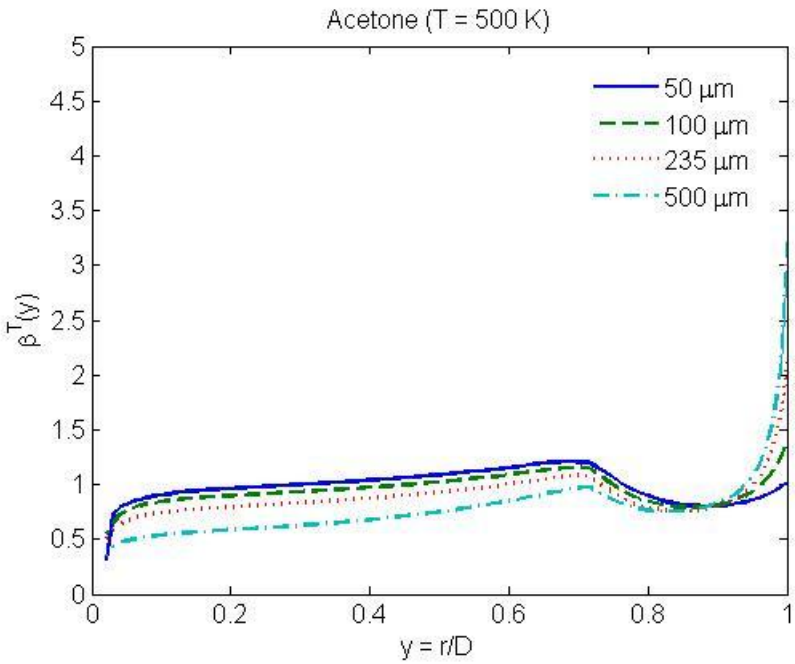

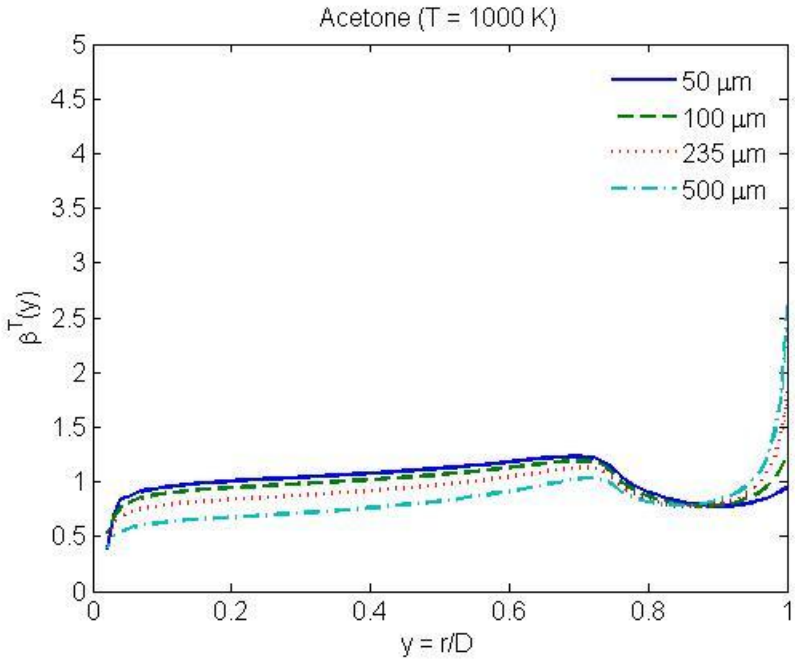

effects of D & T on $\beta^T(y)$

$\beta^T(y)$ – Total local dimensionless volumetric radiation absorption

octane

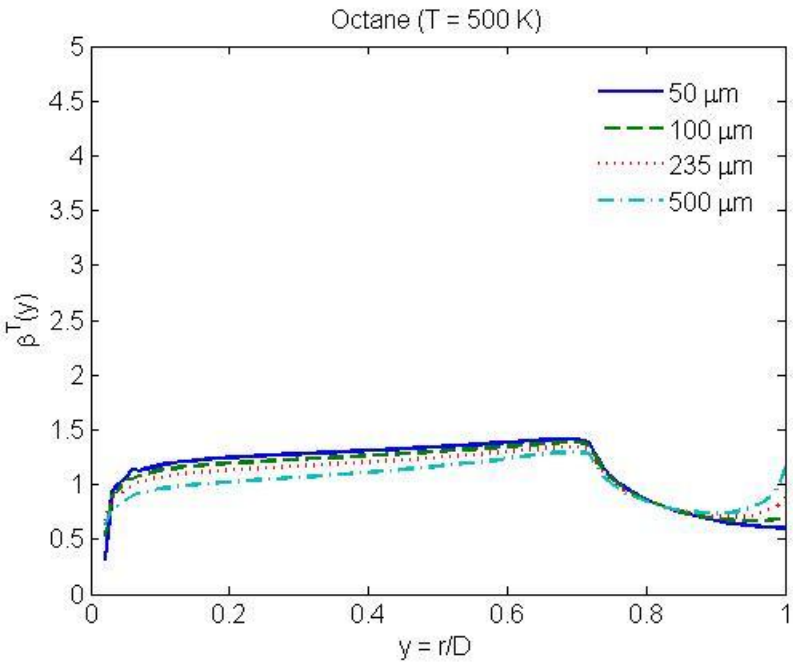

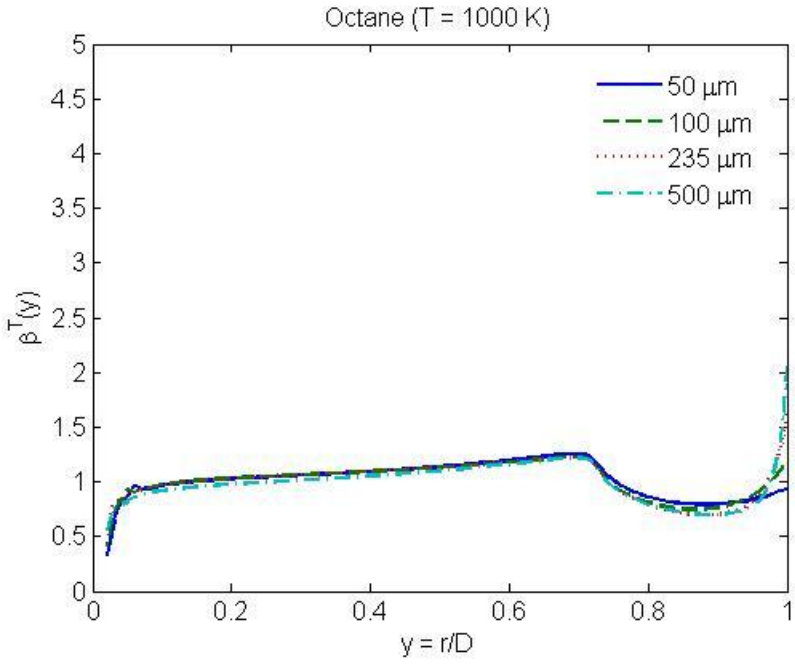

effects of D & T on $\beta^T(y)$

$\beta^T(y)$ – Total local dimensionless volumetric radiation absorption

hexane

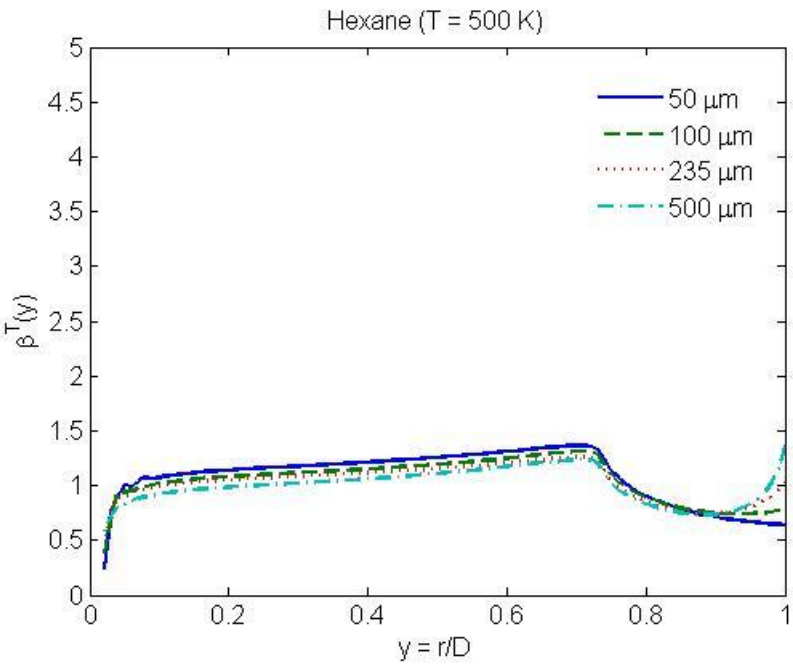

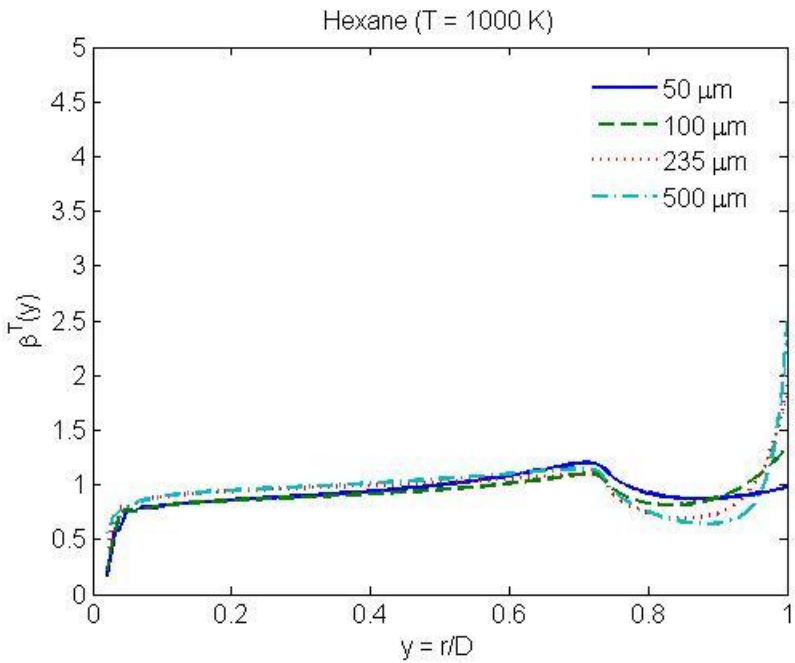

effects of D & T on $\beta^T(y)$

$\beta^T(y)$ – Total local dimensionless volumetric radiation absorption

ethanol

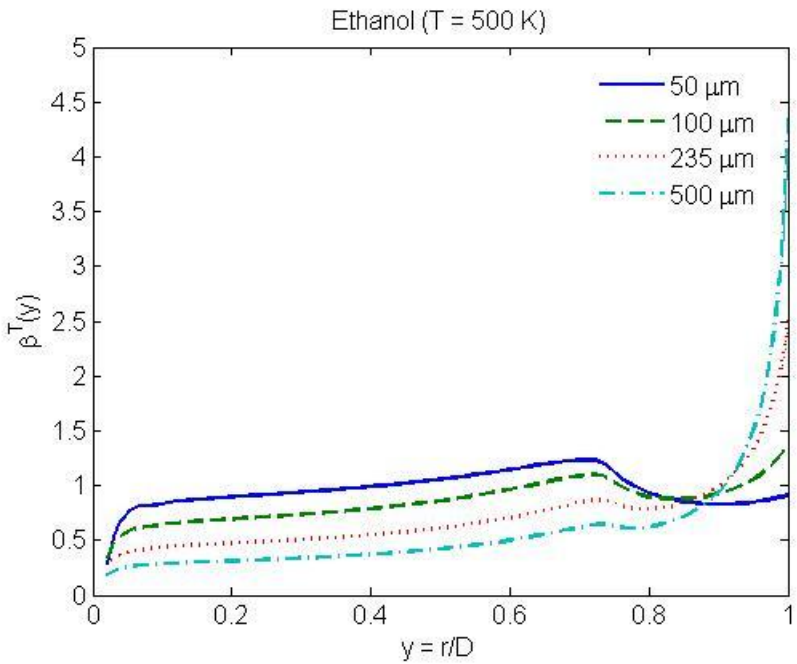

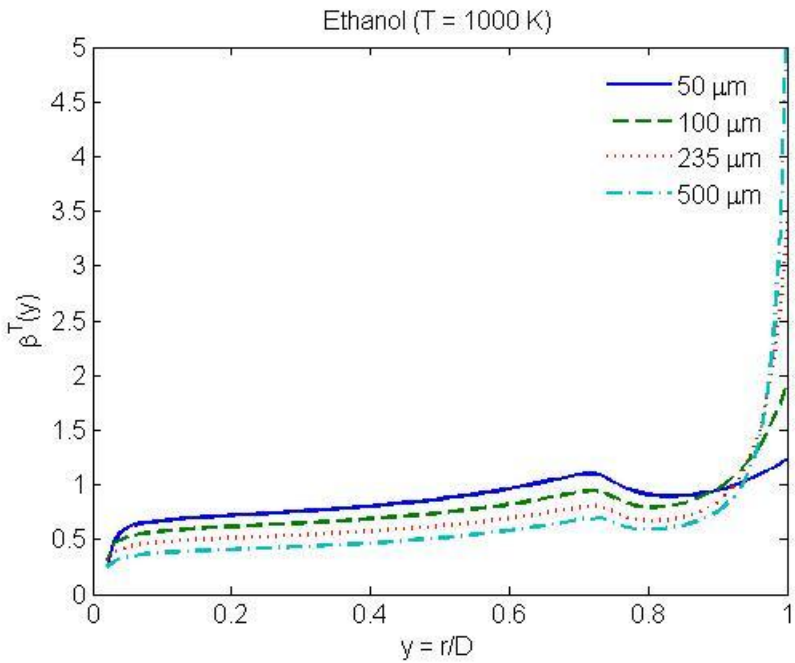

effects of D & T on $\beta^T(y)$

$\beta^T(y)$ – Total local dimensionless volumetric radiation absorption

2-propanol

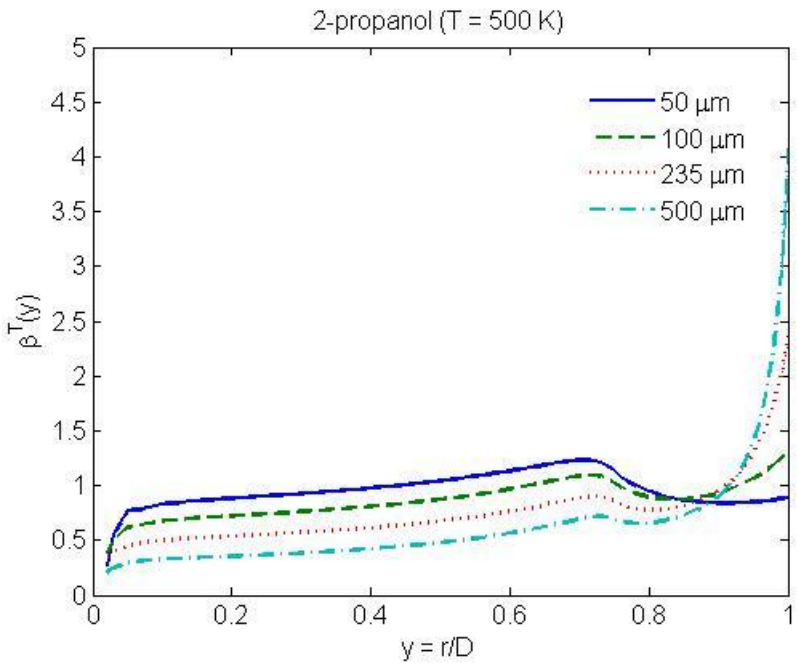

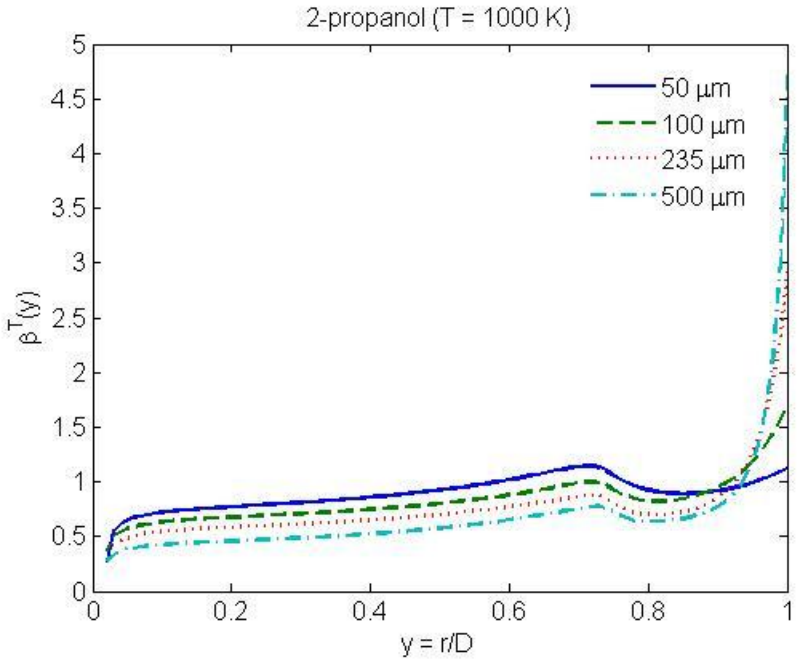

internal radiation absorption distribution

- Temperature change from 500 K to 1000 K significantly affect radiation absorption in hydrocarbons
  - T decreases from 1000 K to 500 K – Peak absorption shifts toward droplet core
- Diameter < 100 μm (all components)
  - Peak absorption shifts toward droplet core

Device	Diameter range (μm)	Wall temperature (K)
Gas turbine	10 – 400	500 – 1000
Typical ICE	20 – 200	450 – 500
Micro gas turbine	20 - 100	600 – 750
Microcombustor	1 - 100	600 - 750

conclusions

Experimental work:

- PLIF successfully implemented to image vapor distribution around droplets
- Highly asymmetric vapor distribution observed for asymmetric radiant heating (asymmetric Stefan flow)
  - not previously reported in the literature

Analytical work:

- Radiation absorption distribution high dependent on *n-k spectrum, diameter* and *irradiation temperature*
- Peak absorption shifts toward droplet interior: $D < 100\ \mu m$
- Hydrocarbon radiation absorption highly sensitive to temperature *(500 – 1000 K)*

implications

- Highly localized vaporization will affect overall vaporization rate
  - Affects eventual combustion of fuel/air mixture
- Fuel rich and fuel lean regions in combustor
  - Longer mixing time with air
- Increased pollutant formation
  - Nitrogen monoxide (lean)
  - Carbon monoxide, hydrocarbons (rich)
- Analytical results used to improve existing combustion models

future work

- ATESR Lab
  - Droplet vaporization under velocity/temperature gradients
  - Collaboration with Dr. Miller (Clemson University) for numerical simulation of current work

Circular Couette Flow Reactor (CCFR)

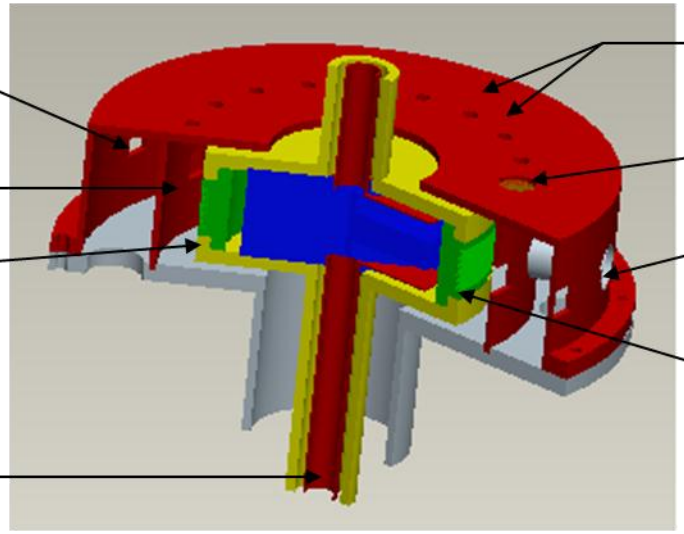

publications

Peer-reviewed publications:

- *Ammigan, K.* and Clack, H.L. (2012), "Comparison of the internal distribution of thermal radiation absorption in liquid droplets of acetone, octane, hexane, ethanol and 2-propanol", **Journal of Quantitative Spectroscopy and Radiative Transfer** (in preparation).

- *Ammigan, K.,* R.S. Miller and H.L. Clack (2011), Effect of asymmetric radiant heating on monodisperse acetone/ethanol and acetone/2-propanol bi-component droplets", **International Journal of Multiphase Flow** 38 (1), pp. 67-72.

- *Ammigan, K.,* R.S. Miller and H.L. Clack (2011), *"Vaporization of bi-component droplets exposed to asymmetric radiant heating*", **Combustion Science and Technology**, 183, pp. 1412 - 1432

- *Ammigan, K.* and H.L. Clack (2009), "*Planar laser-induced fluorescence imaging of the spatial vapor distribution around a monodisperse acetone droplet stream exposed to asymmetric radiant heating*", **Proceedings of the Combustion Institute: 32nd International Symposium** 32 (2), pp. 2179-2186

acknowledgements

- National Science Foundation (Grant No. CTS-0346297)

- Advanced Thermal and Environmental Systems Research Laboratory

  Adviser: Dr. H.L. Clack
  Current and past members: Eric Lee, Peter Bittner, Yasmine Khakpour, Nekheel Gajjar, Vinit Prabhu, Pierre Coutris, Violaine Todoroff

- Dr. Miller (Clemson University)

- Dr. Keefe (Cape Breton University) and Dr. Bertie (University of Alberta)

Questions ?